miR-101-3p suppresses proliferation of orbital fibroblasts by targeting pentraxin-3 in thyroid eye disease

Yanfei Zhu, Yuqing Chen, Xingyi Shu and Ruili Wei

Department of Ophthalmology, Changzheng Hospital of Naval Medical University, Shanghai, China

ABSTRACT

Background: Excessive proliferation of orbital fibroblasts (OFs) is an essential factor in the pathogenesis of thyroid eye disease (TED). While existing evidence indicates that various microRNAs (miRNAs) significantly contribute to TED development, the precise function and targets of miR-101-3p in TED pathogenesis remain unknown. This research aims to elucidate the effects of miR-101-3p on TED-OFs and identify its potential targets.

Methods: Orbital adipose tissues were harvested from both TED patients and healthy controls to culture their fibroblasts. MiR-101-3p mimic or mimic negative control (mimic NC) was transfected into OFs from TED patients, with untreated OFs serving as an additional blank control group. Cell proliferation was assessed using cell counting kit-8 (CCK-8) assay, Ki-67 immunofluorescence staining, and the EdU assay, while apoptosis was evaluated *via* flow cytometry. Quantitative real-time polymerase chain reaction (qRT-PCR) was employed to measure the expression levels of miR-101-3p and pentraxin-3 (PTX3), and PTX3 protein levels were quantified using western blot. A dual-luciferase assay was conducted to ascertain how miR-101-3p and PTX3 interacted.

Results: The results demonstrated a significant downregulation of miR-101-3p in fibroblasts and TED orbital adipose tissues. Transfection with the miR-101-3p mimic upregulated miR-101-3p levels, significantly reducing OFs proliferation without affecting apoptosis. Overexpression of miR-101-3p led to the downregulation of PTX3 in OFs. The dual-luciferase assay validated miR-101-3p binding to PTX3's 3'UTR, thereby repressing its expression. Moreover, overexpression of PTX3 partially rescued the miR-101-3p mimic's inhibitory effect on TED-OFs proliferation.

Conclusion: Our findings illustrate miR-101-3p's role in targeting PTX3 to regulate TED-OFs proliferation, providing novel insights into the pathological mechanisms underlying TED development.

Subjects Biochemistry, Cell Biology, Molecular Biology, Ophthalmology
Keywords Thyroid eye disease, Orbital fibroblasts, MiR-101-3p, Pentraxin-3, Proliferation, Apoptosis

INTRODUCTION

Thyroid eye disease (TED), also known as Graves' ophthalmopathy, manifests as an autoimmune orbital disorder and commonly emerges as an extrathyroidal complication of Graves' disease (*Bahn, 2010*). Patients typically present with a range of symptoms, such as exophthalmos, eyelid retraction, ocular pain, and restrictive strabismus. Notably, exophthalmos stands out as the principal clinical hallmark of TED, primarily attributed to the swelling of adipose and muscular tissues within the orbit. The edematous alterations result from a complex interplay of mechanisms, involving inflammatory cell infiltration, extracellular matrix accumulation, fibroblast proliferation, and adipose tissue expansion (*Longo, Smith & Hegedüs, 2016*). In rare cases, approximately 3% to 5% of patients may encounter vision-threatening conditions, like compressive optic neuropathy or exposed corneal ulcers (*Wiersinga & Bartalena, 2002*). Although significant advancements in elucidating the pathogenesis of TED, a comprehensive understanding of its mechanism remains elusive, presenting ongoing therapeutic challenges and dilemmas (*Taylor et al., 2020*).

Central to TED complex pathogenesis is the critical role of orbital fibroblasts (OFs), which serve as the primary cellular targets in this disorder (*Dik, Virakul & van Steensel, 2016*; *Marinò et al., 2019*). The activation of OFs is a pivotal event in TED pathogenesis, facilitated by interactions with immune cells and their secreted soluble factors (*Huang et al., 2019*). Upon activation, OFs contribute to the inflammatory milieu by producing inflammatory mediators and demonstrate heightened proliferative activity, as well as efficient synthesis of extracellular matrix components, particularly hyaluronan, thereby facilitating tissue expansion, remodeling, and fibrosis in TED (*Bahn, 2010*; *Patel, Yang & Douglas, 2019*). As TED progresses, OFs can further differentiate into adipocytes and myofibroblasts, perpetuating tissue alterations (*Dik, Virakul & van Steensel, 2016*). Notably, the basal proliferative activity of OFs in TED exceeds that of normal OFs (*Kuriyan et al., 2013*). Despite recognizing the significance of OFs in TED pathogenesis, the precise mechanisms underlying their involvement and potential as therapeutic targets remain incompletely elucidated.

MicroRNAs (miRNAs), as short and endogenous noncoding RNAs, play a vital role in physiological regulation by modulating the suppression of target mRNA translation and/or enhancing mRNA degradation (*Bartel, 2009*). Their involvement spans various biological functions, including immune responses, cell proliferation, apoptosis, differentiation, and metabolism (*Martínez-Hernández & Marazuela, 2023*). Recent epigenetic research highlights miRNAs as pivotal regulatory mediators influencing cellular proliferation (*Zhao et al., 2023*; *Wang et al., 2024*), with alterations in their expression tightly linked to fibroblast activation and fibrosis in the heart (*Chang et al., 2024*), liver (*Hao et al., 2024*), lung (*Park et al., 2024*), and kidney (*Rajabi et al., 2024*). Importantly, multiple miRNAs, including miR-103a-3p (*Xie et al., 2023*), miR-146a (*Jang et al., 2018*), miR-155 (*Woeller et al., 2019*), miR-21 (*Lee et al., 2016*), and miR-1287-5p (*Wang et al., 2021*), have been implicated in TED development by affecting OFs proliferation. In a prior microarray profiling study of peripheral blood mononuclear cells from TED patients (*Liu et al., 2023*),

miR-101-3p was identified as significantly dysregulated, making it a compelling candidate for further investigation.

Our decision to focus on miR-101-3p is supported by several key findings. First, bioinformatic network analysis using the miRDB and TargetScan databases predicted pentraxin-3 (PTX3) as a potential target gene of miR-101-3p. PTX3, an acute-phase protein integral to innate immunity, inflammatory responses, and tissue remodeling (*Zhang et al., 2022*), belongs to the long pentraxin family and is expressed across various cell types, including human fibroblasts (*Wang et al., 2015*). Recent studies have highlighted PTX3's involvement in TED, a condition where PTX3 functions as a thyroid-stimulating hormone (TSH)-inducible protein within OFs (*Wang et al., 2015*). TSH receptor signaling in these fibroblasts triggers a complex cascade of molecular events, ultimately influencing cellular behaviors such as growth, proliferation, and extracellular matrix production (*Khong et al., 2016*). In our prior research, elevated PTX3 levels have been observed in orbital tissues and fibroblasts obtained from TED patients (*Wang et al., 2015*; *Mou et al., 2018*), suggesting its involvement in TED-related fibrosis (*Diao et al., 2020*). Given the pivotal role of PTX3 in TED, miR-101-3p was hypothesized to act as a key regulator of PTX3 expression in OFs, thereby modulating proliferative and fibrotic activities.

Furthermore, miR-101-3p has been extensively studied in other diseases, where it has been shown to regulate critical cellular processes such as proliferation, apoptosis, and fibrosis (*Xu et al., 2024*; *Fu, Ye & Hu, 2024*; *Lämmerhirt et al., 2024*). For example, miR-101-3p plays an important role in the regulation of fibrosis in organs like the kidney (*Song et al., 2022*), lung (*Li et al., 2022*), and liver (*Meroni et al., 2019*), where its dysregulation contributes to pathological tissue remodeling. These findings further support the potential relevance of miR-101-3p in TED, as fibroblast activation and fibrosis are key features of the disease.

Although miR-150 has been reported to influence endothelial cell proliferation and migration by targeting PTX3 (*Luo et al., 2018*), the mechanisms underlying the combined involvement of PTX3 and miRNAs in TED progression remain unknown. Therefore, the current study aims to investigate the role of miR-101-3p in TED pathogenesis, focusing on its ability to regulate PTX3 expression and its impact on OFs proliferation. Through this research, we seek to uncover novel molecular mechanisms underlying TED and explore miR-101-3p as a potential therapeutic target for the condition.

MATERIALS AND METHODS

Source of samples

All surgical procedures were performed at Changzheng Hospital's Department of Ophthalmology in Shanghai, China. The study included 10 patients diagnosed with TED (F/M = 5/5, mean age 44.9 ± 12.7 years) who underwent orbital decompressive surgery. These patients were in a stage ranging from moderate to severe or even sight-threatening, with Clinical Activity Scores (CAS) below 3, and had not received glucocorticoid therapy for at least 6 months prior to decompression. Additionally, the control group consisted of 10 healthy volunteers (F/M = 4/6, mean age 43.2 ± 21.8 years) who had blepharoplasty. None of the control subjects had a history of autoimmune thyroid disease or TED.

Table 1 Detailed information of the patients enrolled in the study.

Age, y/Sex	Duration of TED, y	Proptosis (R/L), mm	Smoking	CAS	Disease stage	Surgical treatment
Patients with TED						
49/F	3.2	19/19	No	1/7	Moderate to severe	Orbital decompression
30/M	3.4	18/19	Previous	2/7	Moderate to severe	Orbital decompression
47/F	2	24/23.5	No	1/7	Moderate to severe	Orbital decompression
27/M	5.8	25/23.5	Previous	1/7	Moderate to severe	Orbital decompression
41/M	2	20/24.5	Previous	1/7	Moderate to severe	Orbital decompression
45/F	2.8	20/19	No	2/7	Moderate to severe	Orbital decompression
66/F	1.6	13/15	No	2/7	Sight-threatening	Orbital decompression
32/F	15	22/20	No	0/7	Moderate to severe	Orbital decompression
53/M	2	26/27	Previous	0/7	Moderate to severe	Orbital decompression
59/M	1	16/17	Previous	2/7	Moderate to severe	Orbital decompression
Control patients						
32/F	—	—	No	—	—	Eyelid pouch plasty
53/M	—	—	Previous	—	—	Eyelid pouch plasty
19/F	—	—	No	—	—	Upper lid blepharoplasty
62/M	—	—	Previous	—	—	Eyelid pouch plasty
18/M	—	—	No	—	—	Upper lid blepharoplasty
23/M	—	—	No	—	—	Upper lid blepharoplasty
72/F	—	—	No	—	—	Upper lid blepharoplasty
70/F	—	—	No	—	—	Upper lid blepharoplasty
25/M	—	—	No	—	—	Upper lid blepharoplasty
58/M	—	—	Previous	—	—	Upper lid blepharoplasty

Note:
CAS is a total of 7 points. L, left; R, right; F, female; M, male.

Comprehensive patient details can be found in Table 1. The study protocol was approved by the Committee on Ethics of Biomedicine, Naval Medical University, and we received written informed consent from all participants in the study.

Cell culture

OFs were cultured following established protocols (*Sorisky et al., 1996*). Briefly, orbital adipose tissues were mechanically cut into $2 \times 2 \times 2$ mm fragments and evenly distributed in 10-cm petri dishes. Following tissue adherence, OFs were grown in high-glucose DMEM (Gibco, Waltham, MA, USA) containing 20% FBS, 100 mg/L streptomycin, and 100 U/mL penicillin. Typically, OFs migrated from the tissue explants within 5 days and achieved confluence within 10 days. Subsequently, monolayer cells were passaged with 0.25% trypsin/EDTA (Gibco, Waltham, MA, USA) to establish a continuous cell line. The incubation conditions were set at 37 °C with 5% CO_2 and high humidity to support fibroblast growth. To ensure a constant cell phenotype, three to eight passage cells were used for the subsequent experiments. Each experiment included at least three independent lines of OFs.

Immunofluorescence staining

Cells were seeded on sterile slides in a 24-well plate until the desired confluency was reached. They were then fixed for 15 min with 4% paraformaldehyde and permeabilized for 10 min using 0.1% Triton X-100 (Merck Millipore, MA, USA) in PBS. After blocking with 3% BSA for 30 min, the cells were incubated overnight at 4 °C with primary antibodies. For Ki-67 staining, a primary anti-Ki-67 antibody (Servicebio, Wuhan, China) was used, followed by 1 h incubation at room temperature in the dark with Alexa Fluor 488-conjugated goat anti-mouse IgG (Servicebio, Wuhan, China). Similarly, for vimentin staining, a primary anti-vimentin antibody (Servicebio, Wuhan, China) was used, followed by Alexa Fluor 488-conjugated goat anti-rabbit IgG (Servicebio, Wuhan, China) under the same conditions. Nuclear staining was achieved using mounting medium with DAPI. Fluorescence microscopy (Nikon, Tokyo, Japan) was utilized to examine and capture images of the stained cells, and the number of Ki-67 positive cells was quantified to assess cell proliferation.

Cell transfection and treatment

In our study, miR-101-3p mimic and mimic negative control (mimic NC) were procured from GenePharma (Shanghai, China). At a concentration of 2×10^5 cells per well, cells in the exponential growth phase were carefully seeded onto 6-well plates and allowed to incubate for 24 h before transfection. Lipofectamine^{TM} 2000 (Invitrogen, Carlsbad, CA, USA) was employed for the transfection process, following the manufacturer's protocols precisely. After a 48 h transfection period, we assessed the gene and protein expression profiles in OFs, as well as cell proliferation. The transfection dosage for both the mimic and mimic NC was standardized at 50 nM to ensure optimal transfection efficiency. For recombinant human PTX3 (rhPTX3) (Abcam, Cambridge, UK) treatment, fibroblasts were exposed to 200 ng/mL rhPTX3 in DMEM supplemented with 10% FBS for 24 h.

Quantitative real-time polymerase chain reaction (qRT-PCR)

RNA extraction from tissues or cells was performed using TRIzol reagent (Thermo Fisher Scientific, Waltham, MA, USA), adhering closely to the manufacturer's protocols. RNA concentration and purity were measured through the Nanodrop 2000 spectrophotometer (Thermo Fisher Scientific), ensuring the integrity of subsequent analyses. MiR-101-3p expression levels were examined using the miRNA qRT-PCR detection kit (A2030A001; Biotnt, Shanghai, China), with U6 snRNA serving as the internal reference. Reverse transcription of PTX3 and GAPDH mRNA was executed using the SuperScript$^®$ II Reverse Transcriptase kit (Invitrogen, Carlsbad, CA, USA). Subsequently, PTX3 mRNA levels were detected using the SYBR Green PCR quantitative kit (Invitrogen, Carlsbad, CA, USA), with GAPDH employed as an internal reference. To ensure accuracy and reproducibility, each quantitative PCR reaction was conducted in triplicate. Finally, gene expression levels were calculated utilizing the $2^{-\Delta\Delta \, Ct}$ method, and detailed primer sequences are shown in Table 2.

Table 2 The primer sequences.

Gene name	Sequences (5′ to 3′)
PTX3	Forward: GGCCGAGAACTCGGATGATT
	Reverse: AGCATGCGCTCTCTCATCTG
GAPDH	Forward: GTCTTCACCACCATGGAGAA
	Reverse: TAAGCAGTTGGTGGTGCAG
miR-101-3p	Forward: CCCTACAGTACTGTGATAACTGAA
	Reverse: TCAACTGGTGTCGTGGA
U6	Forward: GCTTCGGCAGCACATAT
	Reverse: ATTTGCGTGTCATCCTTG

Western blot assay

Western blot analysis for PTX3 and β-actin was conducted following established protocols (*Wang et al., 2015*). Quantitative assessment of the Western blots was carried out with Image J software, using β-actin as an internal reference for normalization. We used antibodies purchased from Abcam (Cambridge, UK), specifically the anti-PTX3 antibody (ab125007) and the anti-β-actin antibody (ab8226), to ensure reliability and reproducibility.

5-ethyl-2′-deoxyuridine (EdU) assay

EdU reagents conjugated to Alexa Fluor 594 (Beyotime, Shanghai, China) were used. Cells (2×10^5 per well) were seeded in 6-well plates and incubated overnight at 37 °C with 5% CO_2. The following day, cells were treated with 10 μM EdU and incubated for 2 h to allow for EdU incorporation during DNA synthesis. After incubation, cells were washed three times using the provided wash buffer to remove any residual EdU reagent. EdU detection was performed following the manufacturer's protocol, utilizing the click chemistry reaction to label incorporated EdU with a fluorescent dye. The cells were counterstained with DAPI to visualize nuclei. Fluorescent microscopy was used to capture images, and the proportion of EdU-positive cells was calculated relative to total DAPI-stained cells.

Cell counting kit-8 (CCK-8) assay

After transfection as detailed previously, each cohort of OFs in the exponential growth phase was gathered and distributed into 96-well plates at a density of 2×10^3 cells per well. Cultivation ensued under standard conditions at 37 °C with 5% CO_2. Each experimental condition was replicated in six duplicate wells. Subsequently, cells were cultured for 0, 24, 48, and 72 h. At each specified time point, 10 μL of CCK-8 reagent (Dojindo, Kumamoto, Japan) was added to each well, followed by a 2 h incubation at 37 °C. Optical density (OD) value measurements of each well were then recorded at 450 nm utilizing a microplate reader (MD2; Molecular Devices, San Jose, CA, USA). The resulting cell growth curve was subsequently plotted with time on the x-axis and OD values on the y-axis.

Flow cytometry

Following digestion, the cells were fixed for 2 h at 4 °C using 70% ethanol. After fixation, cells were centrifuged at 1,500 rpm for 5 min with 1 mL PBS, then washed twice. The cells were then again suspended in 100 µL of 1×Binding Buffer that had been chilled ahead. Each tube of cells was supplemented with 5 µL of Annexin V-APC and 5 µL of 7-AAD (Annexin V-APC/7-AAD Apoptosis Detection Kit; Keygen, Shanghai, China), the mixture was carefully mixed and the tubes were incubated for 15 min at room temperature in the dark. After incubation, 400 µL of 1×Binding Buffer that had been chilled ahead was added to each tube. The samples were then analyzed utilizing a NovoCyte 2060R flow cytometer (ACEA Biosciences, Hangzhou, China). Data analysis categorized the cells into live, dead, early apoptotic, and late apoptotic populations, allowing for comparative analysis of apoptotic cell percentages under various experimental conditions.

Bioinformatics analysis

Bioinformatics analysis serves as a powerful tool for studying miRNA functions. Employing the miRDB (http://www.mirdb.org/) and TargetScan database (https://www.targetscan.org/vert_80/), the binding sites of miR-101-3p within the PTX3 3'UTR were predicted.

Dual-luciferase assay

Based on bioinformatics predictions, the binding sites' wild-type (WT) and mutant (MUT) sequences (PTX3 3'UTR-WT and PTX3 3'UTR-MUT) were created, synthesized, and cloned into a luciferase reporter vector (OBiO Tech, Shanghai, China). Following that, 293T cells were co-transfected with these constructs and either miR-101-3p mimic (100 nM) or mimic NC (100 nM). Using a dual-luciferase assay kit (Promega, Fitchburg, WI, USA), luciferase activity was assessed after the cells were cultivated 48 h. The relative luciferase activity was assessed by calculating the ratio of Firefly luciferase activity to Renilla luciferase activity, which served as the internal reference.

Statistical analysis

Data analysis and visualization were carried out with GraphPad Prism (version 9; GraphPad Software, La Jolla, CA, USA), with results presented as mean ± standard deviation. Comparisons between two groups were conducted using the t-test, while comparisons among multiple groups were performed using one-way analysis of variance (ANOVA). $P < 0.05$ was considered statistically significant.

RESULTS

Immunofluorescence detection of orbital fibroblasts

To identify OFs, vimentin antibodies were used and observed with a laser scanning confocal microscope. Under microscopic examination, OFs isolated from human subjects displayed spindle or irregular shapes, a transparent cytoplasm, and a large surface area. The cells were densely packed, exhibiting overlapping growth patterns. Immunofluorescence analysis revealed positive expression of the vimentin antigen in OFs,

with a purity exceeding 90% (Fig. 1). These results indicate that the cultured OFs possessed adequate purity for subsequent experimental procedures.

miR-101-3p was notably downregulated in TED orbital adipose tissues and OFs

To validate alterations in miR-101-3p expression within orbital adipose tissues of individuals with TED, we enrolled a cohort of 20 participants, comprising 10 patients diagnosed with TED and 10 healthy controls. Detailed clinical information for these individuals is listed in Table 1. No significant differences in age or gender were observed between the two cohorts. Subsequently, the expression levels of miR-101-3p were assessed using qRT-PCR, revealing a noteworthy reduction in miR-101-3p expression within orbital adipose tissues of TED patients compared to controls (Fig. 2A). Moreover, miR-101-3p expression was evaluated in OFs obtained from normal ($n = 6$) and TED ($n = 6$) tissues, exhibiting a consistent downregulation pattern in OFs from TED tissues compared to those from healthy controls (Fig. 2B). Taken together, these findings indicate a marked reduction in miR-101-3p expression within both orbital adipose tissues and OFs derived from individuals with TED.

Overexpressed miR-101-3p suppressed proliferation of TED-OFs

To assess the impact of miR-101-3p on TED-OFs, cells were transfected with miR-101-3p mimic or mimic NC, and transfection efficiency was confirmed *via* qRT-PCR, showing a significant increase in miR-101-3p levels in the mimic group (Fig. 3A). Using the CCK-8 assay, a marked decrease in cell viability was observed in the miR-101-3p mimic group (Fig. 3B). Specifically, the mimic NC group, serving as the control, exhibited absorbance values at OD450 nm wavelength of 0.84 ± 0.05, whereas miR-101-3p mimic group displayed values of 0.61 ± 0.04 at 72 h. Furthermore, immunofluorescence analysis was conducted to assess the localization and expression of proliferation marker Ki-67 in cultured OFs. Comparisons showed the proportion of Ki-67-positive cells was notably reduced in the miR-101-3p mimic group, indicating suppressed proliferation (Fig. 3C). To further confirm this effect, an EdU assay was performed, which showed results consistent with the Ki-67 immunofluorescence findings. The EdU-positive cells were notably lower in the miR-101-3p mimic group (Fig. 3D). Finally, to explore whether cell apoptosis correlates with OFs growth inhibition induced by miR-101-3p, we assessed apoptosis in OFs with Annexin V-APC and 7-AAD staining *via* flow cytometry. Unexpectedly, analysis showed no significant difference in cell apoptosis between those transfected with miR-101-3p mimic and mimic NC group (Fig. 3E). These results suggest that miR-101-3p may act as an inhibitor of TED-OFs proliferation without inducing apoptosis.

miR-101-3p directly targeted PTX3 and suppressed PTX3 expression

It is widely recognized that miRNAs function by targeting downstream genes. To elucidate the mechanism underlying miR-101-3p involvement in TED pathogenesis, we employed the online tool miRDB and TargetScan to predict its potential targets, identifying a highly conserved binding sequence between miR-101-3p and PTX3 3'UTR among the candidate
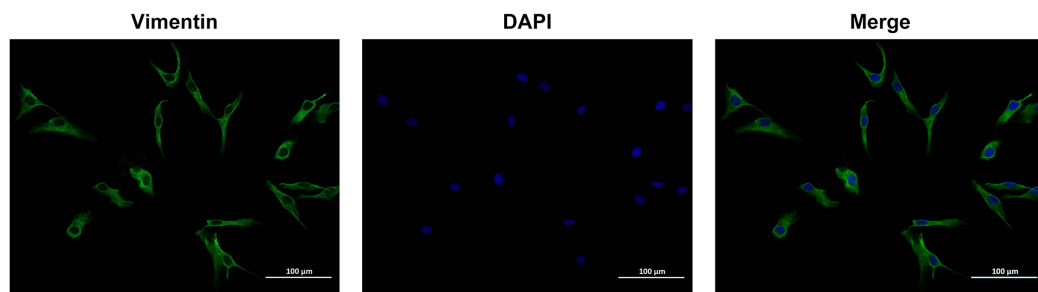
Figure 1 Identification of Vimentin protein by immunofluorescence method. Images were taken at 200× magnification, scale bars = 100 μm.   Full-size ◩ DOI: 10.7717/peerj.18535/fig-1
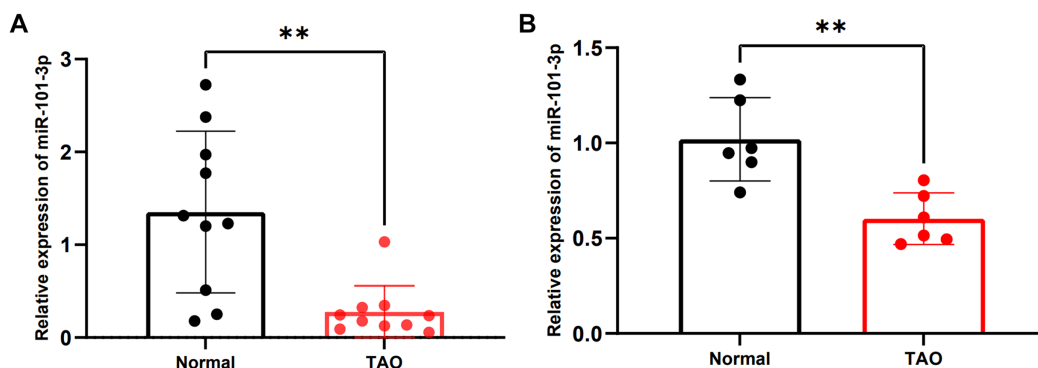

Figure 2 miR-101-3p was notably downregulated in TED orbital adipose tissues and OFs. (A) miR-101-3p expression was evaluated using qRT-PCR in orbital tissues from 10 TED patients and 10 normal controls. (B) miR-101-3p expression was analyzed in OFs derived from orbital tissues of normal subjects ($n = 6$) and TED donors ($n = 6$). Relative quantification was standardized to U6. Data are presented as mean ± SD. **$P < 0.01$ Full-size ◩ DOI: 10.7717/peerj.18535/fig-2

genes (Fig. 4A). Subsequently, the impact of miR-101-3p on PTX3 mRNA expression and protein levels was investigated. As depicted in Figs. 4B and 4C, transfection with miR-101-3p mimic significantly reduced PTX3 mRNA and protein expression. Additionally, we evaluated PTX3 mRNA expression levels in 10 TED orbital adipose tissues and 10 normal samples, revealing a significant upregulation of PTX3 mRNA expression in TED orbital tissues (Fig. 4D). Furthermore, we observed a negative correlation between PTX3 and miR-101-3p expression in both TED and normal orbital tissues (Fig. 4E). Moreover, PTX3 3'UTR-WT and PTX3 3'UTR-MUT luciferase reporter plasmids were constructed and used in a dual-luciferase assay to confirm the binding of miR-101-3p to PTX3. The results demonstrated that PTX3 3'UTR-WT luciferase activity was significantly suppressed by co-transfection with the miR-101-3p mimic. However, cells co-transfected with the miR-101-3p mimic and PTX3 3'UTR-MUT showed no significant changes in luciferase activity (Fig. 4F). Collectively, these results indicate that miR-101-3p binds to PTX3 and inhibits PTX3 expression.

miR-101-3p suppressed TED-OFs proliferation by targeting PTX3

In light of our previous experiments demonstrating the direct modulation of PTX3 by miR-101-3p, we formulated an assumption: miR-101-3p inhibits TED-OFs proliferation
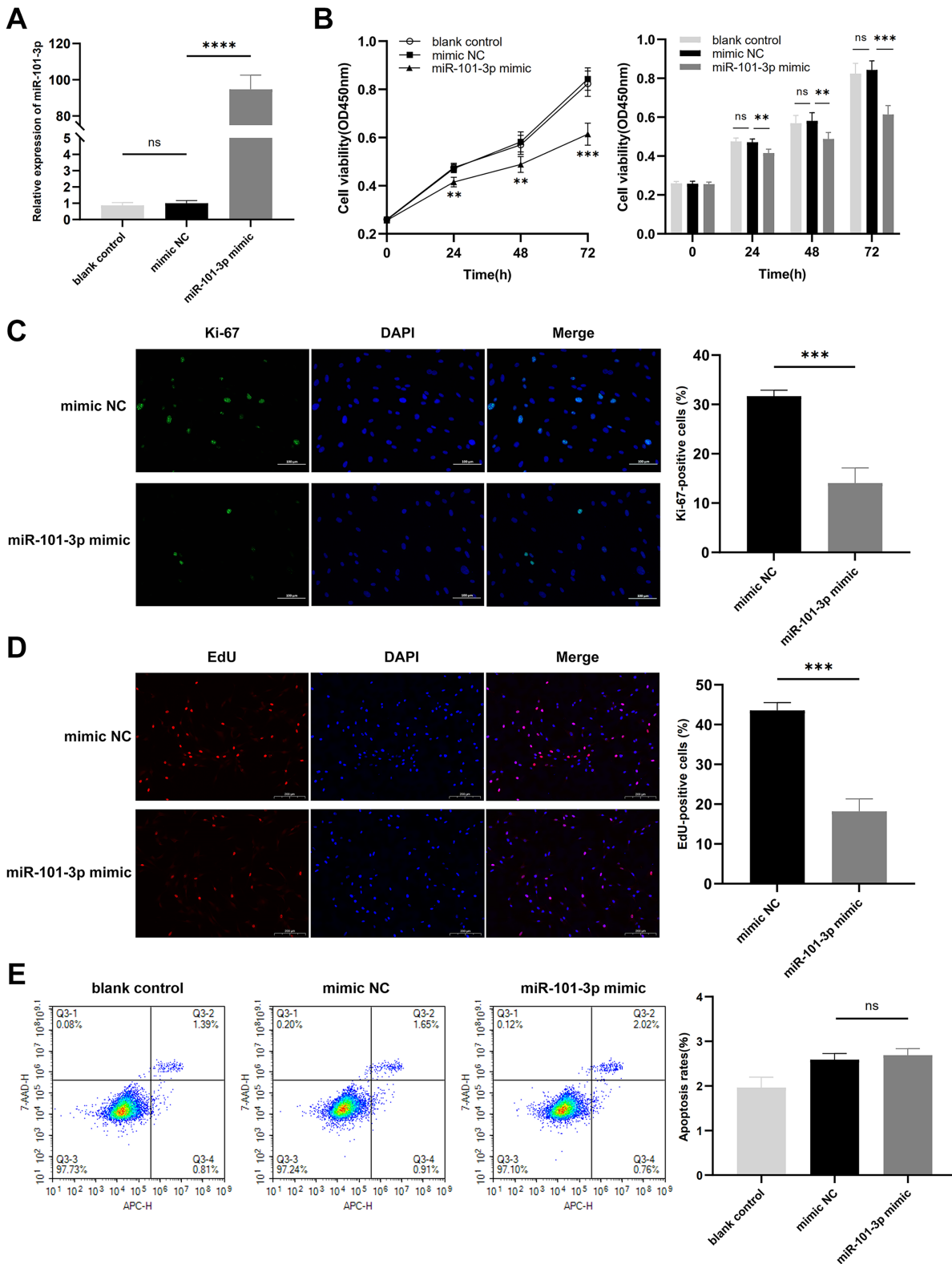
Figure 3 Overexpressed miR-101-3p suppressed TED-OFs proliferation without affecting apoptosis. (A) miR-101-3p overexpression in TED-OFs was confirmed *via* qRT-PCR after transfection with miR-101-3p mimic. (B) TED-OFs transfected with miR-101-3p mimic were assessed for cell viability using the CCK-8 assay at specified time points. (C) Immunofluorescence staining was used to examine the intranuclear distribution

Figure 4 **miR-101-3p directly targeted PTX3 and suppressed PTX3 expression.** (A) Interaction of miR-101-3p with PTX3 3'UTR-WT and PTX3 3'UTR-MUT. (B and C) After transfection with miR-101-3p mimic or mimic NC, TED-OFs were analyzed for PTX3 mRNA expression using qRT-PCR and for protein levels using immunoblotting. (D) PTX3 mRNA expression in orbital tissues from both TED patients and normal controls was assessed *via* qRT-PCR. (E) Pearson's correlation analysis was used to assess the relationship between PTX3 and miR-101-3p expression in orbital adipose tissues. (F) The dual-luciferase assay indicated that the miR-101-3p mimic reduced luciferase activity when PTX3 3'UTR-WT was co-transfected into 293T cells, but not with the PTX3 3'UTR-MUT vector. Data are presented as mean ± SD. Three biological replicates, **$P < 0.01$, ns was considered as non-significant.
Full-size ⬚ DOI: 10.7717/peerj.18535/fig-4

by directly targeting PTX3. To test whether overexpression of PTX3 could antagonize the effects of miR-101-3p on cell proliferation, we stimulated miR-101-3p-overexpressing TED-OFs for 24 h with exogenous rhPTX3 (200 ng/mL). As expected, the miR-101-3p mimic reduced PTX3 protein levels, but this effect was reversed upon rhPTX3 treatment, which significantly increased PTX3 expression (Fig. 5A). Importantly, qRT-PCR analysis confirmed that miR-101-3p expression remained similar between the mimic and the mimic+rhPTX3 groups, indicating that rhPTX3 specifically reversed the protein-level effects without altering miR-101-3p expression itself (Fig. 5B). Consistent with earlier findings, CCK-8 assays showed that miR-101-3p overexpression significantly reduced cell viability, while rhPTX3 supplementation partially rescued this effect (Fig. 5C). Furthermore, immunofluorescence analysis of Ki-67 revealed fewer proliferating cells in the miR-101-3p mimic group, but rhPTX3 treatment restored Ki-67 expression (Fig. 5D). Similarly, the EdU assay, which provides a more direct measure of DNA synthesis, showing fewer EdU-positive cells in the miR-101-3p mimic group, which was partially reversed by rhPTX3 supplementation (Fig. 5E). Overall, these results demonstrate that miR-101-3p suppresses TED-OFs proliferation by directly targeting PTX3, and that restoring PTX3 levels can counterbalance miR-101-3p's inhibitory effects.

DISCUSSION

Recent research has increasingly focused on the epigenetic mechanisms of TED, particularly emphasizing the role of miRNAs (Shahraki et al., 2023). By binding to messenger RNAs, miRNAs affect the expression of target genes and the development of disease (Bartel, 2009). The malignant progression of TED may be driven by changes in miRNA expression, with miRNA levels in TED patients differing according to their CAS (Wei et al., 2014). MiRNAs also play a crucial role in predicting treatment outcomes and influencing the clinical manifestations of TED (Shen et al., 2015; Martínez-Hernández et al., 2018). In this research, we found a significant reduction of miR-101-3p in TED orbital tissue samples and fibroblasts. While PTX3 mRNA was upregulated in TED orbital tissue samples, consistent with our previous study (Mou et al., 2018). MiR-101-3p directly targeted PTX3, and its overexpression inhibited TED-OFs proliferation. Importantly, we confirmed this anti-proliferative effect through three independent methods: CCK-8 assay, Ki-67 immunofluorescence, and EdU assay. Additionally, supplementation with rhPTX3 reversed the miR-101-3p mimic's inhibition of PTX3 expression and cell proliferation. The findings indicate that elucidating miRNA expression alterations in TED can deepen our understanding of its pathogenesis and provide new diagnostic and therapeutic avenues.

Excessive proliferation of OFs is a hallmark feature of TED and drives further disease progression (Kuriyan, Phipps & Feldon, 2008). As the number of fibroblasts increases within the orbit, their capacity to fuel orbital remodeling escalates, characterized by sustained activation and heightened production of hyaluronan and inflammatory mediators (Dik, Virakul & van Steensel, 2016; Khong et al., 2016). Moreover, fibroblasts can differentiate into adipocytes or myofibroblasts, thereby exacerbating TED progression (Dik, Virakul & van Steensel, 2016; Kuriyan et al., 2013). In fact, multiple miRNAs have been implicated in TED development by affecting OFs activation. For example, miR-103a-
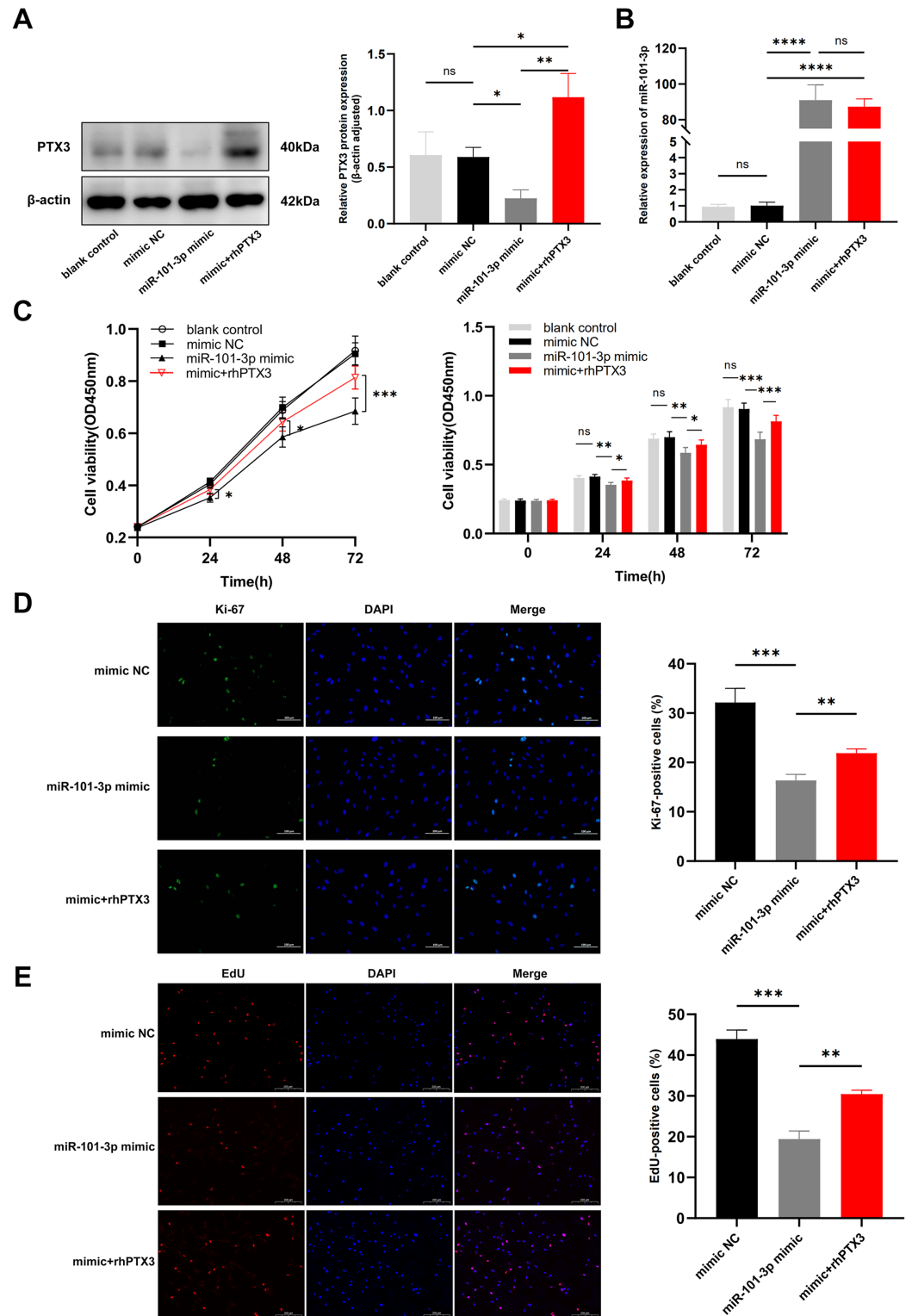
Figure 5 miR-101-3p suppressed TED-OFs proliferation by targeting PTX3. (A) PTX3 protein levels in transfected TED-OFs (blank control, mimic NC, miR-101-3p mimic, and mimic+rhPTX3). (B) miR-101-3p expression in transfected TED-OFs was assessed *via* qRT-PCR. (C) The proliferative ability of TED-OFs was detected by CCK-8 assay. (D) Immunofluorescence staining was used to examine the intranuclear distribution and expression of Ki-67 in TED-OFs. Images were taken at 200× magnification,

Figure 5 (continued)
scale bars = 100 μm. The bar graph shows the mean ratio of Ki-67-positive cells for each group. (E) EdU staining evaluated the proportion of EdU-positive cells in TED-OFs. Images were taken at 200× magnification, scale bars = 200 μm. Data are presented as mean ± SD. Three biological replicates, *$P < 0.05$, **$P < 0.01$, ***$P < 0.001$, ****$P < 0.0001$, ns was considered as non-significant.

Full-size ☑ DOI: 10.7717/peerj.18535/fig-5

3p was identified as overexpressed in TED orbital tissues and fibroblasts, promoting OFs activation and orbital fibrosis (*Xie et al., 2023*). Similarly, miR-155 and miR-146a enhance the proliferation of TED-OFs by suppressing target genes that inhibit cell proliferation (*Woeller et al., 2019*). Aligns with previous research, miR-101-3p expression has been noted in various tumors and tumor cell lines, correlating with its role in regulating cell proliferation (*Lämmerhirt et al., 2024*; *Gao et al., 2024*; *Sun et al., 2024*). This implies that the decreased levels of miR-101-3p may contribute to the abnormal proliferation of fibroblasts observed in TED.

However, few reports have focused on the role of miRNAs in regulating TED-OFs apoptosis. Given that miR-101-3p has been shown to promote apoptosis in several tumor cells (*Lämmerhirt et al., 2024*; *Gao et al., 2024*), we hypothesized that modulation of miR-101-3p expression could induce changes in TED-OFs apoptosis. Unexpectedly, flow cytometry analysis did not reveal increased apoptosis in TED-OFs transfected with the miR-101-3p mimic (Fig. 3E). This result suggests that the effect of miR-101-3p on apoptosis may be context-dependent, with TED-OFs exhibiting unique signaling pathways or characteristics that alter their sensitivity to miR-101-3p-mediated apoptosis. Relying solely on the CCK-8 assay made it difficult to determine if reduced cell viability was due to decreased proliferation or increased apoptosis. Therefore, the flow cytometry results indicate that the decline in cell activation is attributed to decreased proliferation rather than increased apoptosis. It's also important to note that no apoptosis-inducing agent was used as a positive control in this study. Including a positive control would have confirmed the sensitivity of our assay and provided a more thorough evaluation of miR-101-3p's role in apoptosis. Future studies should incorporate such controls to better assess this aspect.

Mechanistically, miRNAs function by binding to and regulating the expression of downstream mRNAs. In our study, dual-luciferase assay identified PTX3 as a target for miR-101-3p. PTX3, a member of the long pentraxin subfamily, has been reported to promote cell proliferation. For instance, increased expression of PTX3 promotes proliferation and differentiation in human osteoblasts (*Greggi et al., 2021*). Moreover, in desmoid tumors, PTX3 secretion from nonmutant fibroblastic cells has been shown to stimulate mutant cell proliferation *via* STAT6 activation (*Al-Jazrawe et al., 2023*). Building on our previous findings suggesting a potential link between PTX3 and the pathological mechanism of TED (*Mou et al., 2018*; *Diao et al., 2020*), we sought to explore how PTX3 influences the proliferation of TED-OFs. Here, we show that PTX3 overexpression partially reversed the inhibitory effect of miR-101-3p overexpression on TED-OFs proliferation (Figs. 5C–5E), indicating that miR-101-3p regulates OFs proliferation by

targeting PTX3. This might partially account for the excessive proliferation of OFs observed in TED.

Indeed, miR-101-3p likely targets other mRNAs in addition to PTX3, as miRNAs generally have multiple targets. Several studies have reported that miR-101-3p suppresses tumor cell proliferation by directly targeting EZH2 (*Chen et al., 2022*; *Dong et al., 2021*; *Xue et al., 2022*). In early-onset preeclampsia, upregulation of miR-101-3p decreases VEGFA expression, thereby inhibiting trophoblast cell proliferation (*Li et al., 2023*). Thus, miR-101-3p may modulate multiple genes during the activation process of OFs in TED, not solely targeting PTX3. Additionally, miR-101-3p might have other significant roles in TED pathophysiology. In diabetic retinopathy, it regulates VEGFA expression, stimulating angiogenesis and inflammatory responses (*Fu, Ye & Hu, 2024*). Downregulation of miR-101-3p exacerbates inflammation by targeting MAPK1 in systemic lupus erythematosus (*Zhao et al., 2021*). Moreover, miR-101-3p is pivotal in the protective effect of Dexmedetomidine against kidney fibrosis in diabetic mice (*Song et al., 2022*). Thus, miR-101-3p could potentially exert a profound influence on cell proliferation, inflammatory signaling, and fibrosis, consequently impacting orbital tissue remodeling in TED.

While OFs play a crucial role in the pathogenesis of TED, the disease also involves contributions from various immune cell types (*Lehmann et al., 2008*). However, the specific impact of miR-101-3p on other immune cells in TED remains poorly understood. Furthermore, TED tissues were obtained from orbital decompression surgeries, whereas non-TED tissues were harvested from upper eyelid blepharoplasty. Although obtaining non-TED orbital tissue is exceedingly rare, the use of eyelid tissue as a control is a more feasible approach given the practical limitations. Nevertheless, this may introduce some differences in fibroblast behavior due to the distinct origins of the tissues. Despite these limitations, this research is the first to demonstrate that miR-101-3p targets PTX3 and highlights its potential role in regulating TED-OFs proliferation. Future studies using animal models or other methods of obtaining appropriate controls will further clarify the role of miR-101-3p in TED pathogenesis.

CONCLUSIONS

In conclusion, our research highlights the regulatory role of the miR-101-3p/PTX3 axis in TED-OFs proliferation. As clinical trials of miRNA-based therapeutics for diverse types of cancer increase (*Seyhan, 2024*), our findings offer a potential novel target for TED therapy. Developing a safe delivery system for miRNAs into fibroblasts is imperative for advancing TED treatment.

ADDITIONAL INFORMATION AND DECLARATIONS

Competing Interests

The authors declare that they have no competing interests.

Author Contributions

- Yanfei Zhu conceived and designed the experiments, performed the experiments, analyzed the data, prepared figures and/or tables, authored or reviewed drafts of the article, and approved the final draft.
- Yuqing Chen conceived and designed the experiments, prepared figures and/or tables, and approved the final draft.
- Xingyi Shu performed the experiments, analyzed the data, prepared figures and/or tables, and approved the final draft.
- Ruili Wei conceived and designed the experiments, authored or reviewed drafts of the article, and approved the final draft.

Human Ethics

The following information was supplied relating to ethical approvals (*i.e.*, approving body and any reference numbers):

The study protocol was approved by the Committee on Ethics of Biomedicine, Naval Medical University.

Data Availability

The following information was supplied regarding data availability:

The raw measurements are available in the Supplemental Files.

Supplemental Information

Supplemental information for this article can be found online at http://dx.doi.org/10.7717/peerj.18535#supplemental-information.

REFERENCES

Al-Jazrawe M, Xu S, Poon R, Wei Q, Przybyl J, Varma S, van de Rijn M, Alman BA. 2023. CD142 identifies neoplastic desmoid tumor cells, uncovering interactions between neoplastic and stromal cells that drive proliferation. *Cancer Research Communications* **3(4)**:697–708 DOI 10.1158/2767-9764.CRC-22-0403.

Bahn RS. 2010. Graves' ophthalmopathy. *New England Journal of Medicine* **362(8)**:726–738 DOI 10.1056/NEJMra0905750.

Bartel DP. 2009. MicroRNAs: target recognition and regulatory functions. *Cell* **136(2)**:215–233 DOI 10.1016/j.cell.2009.01.002.

Chang W, Xiao D, Fang X, Wang J. 2024. Oxidative modification of miR-30c promotes cardiac fibroblast proliferation via CDKN2C mismatch. *Scientific Reports* **14**:13085 DOI 10.1038/s41598-024-63635-2.

Chen Z, Lin X, Wan Z, Xiao M, Ding C, Wan P, Li Q, Zheng S. 2022. High expression of EZH2 mediated by ncRNAs correlates with poor prognosis and tumor immune infiltration of hepatocellular carcinoma. *Genes* **13(5)**:876 DOI 10.3390/genes13050876.

Diao J, Chen X, Jiang L, Mou P, Wei R. 2020. Transforming growth factor-β1 suppress pentraxin-3 in human orbital fibroblasts. *Endocrine* **70(1)**:78–84 DOI 10.1007/s12020-020-02307-3.

Dik WA, Virakul S, van Steensel L. 2016. Current perspectives on the role of orbital fibroblasts in the pathogenesis of Graves' ophthalmopathy. *Experimental Eye Research* **142**:83–91 DOI 10.1016/j.exer.2015.02.007.

Dong Y, Gao Y, Xie T, Liu H, Zhan X, Xu Y. 2021. miR-101-3p serves as a tumor suppressor for renal cell carcinoma and inhibits its invasion and metastasis by targeting EZH2. *BioMed Research International* **2021(7)**:9950749 DOI 10.1155/2021/9950749.

Fu W, Ye Y, Hu F. 2024. LncRNA XIST promotes neovascularization in diabetic retinopathy by regulating miR-101-3p/VEGFA. *Archives of Endocrinology and Metabolism* **68(4)**:e230097 DOI 10.20945/2359-4292-2023-0097.

Gao H, Gao Z, Liu X, Sun X, Hu Z, Song Z, Zhang C, Fei J, Wang X. 2024. miR-101-3p-mediated role of PDZK1 in hepatocellular carcinoma progression and the underlying PI3K/Akt signaling mechanism. *Cell Division* **19(1)**:9 DOI 10.1186/s13008-023-00106-6.

Greggi C, Cariati I, Onorato F, Iundusi R, Scimeca M, Tarantino U. 2021. PTX3 effects on osteogenic differentiation in osteoporosis: an in vitro study. *International Journal of Molecular Sciences* **22(11)**:5944 DOI 10.3390/ijms22115944.

Hao Y, Song S, Li T, Zai Q, Ma N, Li Y, Yang L, Xiao P, Xu T, Ji L, Tan J, Ahmed YA, Xiang X, Wang X, Lafdil F, Xie Q, He Y. 2024. Oxidative stress promotes liver fibrosis by modulating the microRNA-144 and SIN3A-p38 pathways in hepatic stellate cells. *International Journal of Biological Sciences* **20(7)**:2422–2439 DOI 10.7150/ijbs.92749.

Huang Y, Fang S, Li D, Zhou H, Li B, Fan X. 2019. The involvement of T cell pathogenesis in thyroid-associated ophthalmopathy. *Eye (London, England)* **33(2)**:176–182 DOI 10.1038/s41433-018-0279-9.

Jang SY, Park SJ, Chae MK, Lee JH, Lee EJ, Yoon JS. 2018. Role of microRNA-146a in regulation of fibrosis in orbital fibroblasts from patients with Graves' orbitopathy. *The British Journal of Ophthalmology* **102(3)**:407–414 DOI 10.1136/bjophthalmol-2017-310723.

Khong JJ, McNab AA, Ebeling PR, Craig JE, Selva D. 2016. Pathogenesis of thyroid eye disease: review and update on molecular mechanisms. *The British Journal of Ophthalmology* **100(1)**:142–150 DOI 10.1136/bjophthalmol-2015-307399.

Kuriyan AE, Phipps RP, Feldon SE. 2008. The eye and thyroid disease. *Current Opinion in Ophthalmology* **19(6)**:499–506 DOI 10.1097/ICU.0b013e3283131557.

Kuriyan AE, Woeller CF, O'Loughlin CW, Phipps RP, Feldon SE. 2013. Orbital fibroblasts from thyroid eye disease patients differ in proliferative and adipogenic responses depending on disease subtype. *Investigative Ophthalmology & Visual Science* **54(12)**:7370–7377 DOI 10.1167/iovs.13-12741.

Lämmerhirt L, Kappelmann-Fenzl M, Fischer S, Meier P, Staebler S, Kuphal S, Bosserhoff AK. 2024. Loss of miR-101-3p in melanoma stabilizes genomic integrity, leading to cell death prevention. *Cellular & Molecular Biology Letters* **29(1)**:29 DOI 10.1186/s11658-024-00552-2.

Lee JY, Yun M, Paik JS, Lee SB, Yang SW. 2016. PDGF-BB enhances the proliferation of cells in human orbital fibroblasts by suppressing PDCD4 expression via up-regulation of microRNA-21. *Investigative Ophthalmology & Visual Science* **57(3)**:908–913 DOI 10.1167/iovs.15-18157.

Lehmann GM, Feldon SE, Smith TJ, Phipps RP. 2008. Immune mechanisms in thyroid eye disease. *Thyroid: Official Journal of the American Thyroid Association* **18(9)**:959–965 DOI 10.1089/thy.2007.0407.

Li Q, Li S, Ding J, Pang B, Li R, Cao H, Ling L. 2023. MALAT1 modulates trophoblast phenotype via miR-101-3p/VEGFA axis. *Archives of Biochemistry and Biophysics* **744**:109692 DOI 10.1016/j.abb.2023.109692.

Li C, Xia J, Yao W, Yang G, Tian Y, Qi Y, Hao C. 2022. Mechanism of LncRNA XIST/ miR-101-3p/ZEB1 axis in EMT associated with silicosis. *Toxicology Letters* **360**:11–19 DOI 10.1016/j.toxlet.2022.03.001.

Liu R, Ye Z, Liu Q, Xuan M, Li R, Zhang L, Zhang K, Fang P, Xue Y. 2023. MicroRNA-376b is involved in the pathogenesis of thyroid-associated ophthalmopathy by regulating HAS2. *Endocrine* **82(1)**:87–95 DOI 10.1007/s12020-023-03382-y.

Longo DL, Smith TJ, Hegedüs L. 2016. Graves' disease. *The New England Journal of Medicine* **375(16)**:1552–1565 DOI 10.1056/NEJMra1510030.

Luo XY, Zhu XQ, Li Y, Wang XB, Yin W, Ge YS, Ji WM. 2018. MicroRNA-150 restores endothelial cell function and attenuates vascular remodeling by targeting PTX3 through the NF-κB signaling pathway in mice with acute coronary syndrome. *Cell Biology International* **42(9)**:1170–1181 DOI 10.1002/cbin.10985.

Marinò M, Rotondo Dottore G, Ionni I, Lanzolla G, Sabini E, Ricci D, Sframeli A, Mazzi B, Menconi F, Latrofa F, Vitti P, Marcocci C, Chiovato L. 2019. Serum antibodies against the insulin-like growth factor-1 receptor (IGF-1R) in Graves' disease and Graves' orbitopathy. *Journal of Endocrinological Investigation* **42(4)**:471–480 DOI 10.1007/s40618-018-0943-8.

Martínez-Hernández R, Marazuela M. 2023. MicroRNAs in autoimmune thyroid diseases and their role as biomarkers. *Best Practice & Research Clinical Endocrinology & Metabolism* **37(2)**:101741 DOI 10.1016/j.beem.2023.101741.

Martínez-Hernández R, Sampedro-Núñez M, Serrano-Somavilla A, Ramos-Leví AM, de la Fuente H, Triviño JC, Sanz-García A, Sánchez-Madrid F, Marazuela M. 2018. A MicroRNA signature for evaluation of risk and severity of autoimmune thyroid diseases. *The Journal of Clinical Endocrinology and Metabolism* **103(3)**:1139–1150 DOI 10.1210/jc.2017-02318.

Meroni M, Longo M, Erconi V, Valenti L, Gatti S, Fracanzani AL, Dongiovanni P. 2019. mir-101-3p downregulation promotes fibrogenesis by facilitating hepatic stellate cell transdifferentiation during insulin resistance. *Nutrients* **11(11)**:2597 DOI 10.3390/nu11112597.

Mou P, Chen Z, Jiang L, Cheng J, Wei R. 2018. PTX3: a potential biomarker in thyroid associated ophthalmopathy. *BioMed Research International* **2018**:5961974 DOI 10.1155/2018/5961974.

Park JS, Kim C, Choi J, Jeong HY, Moon YM, Kang H, Lee EK, Cho ML, Park SH. 2024. MicroRNA-21a-5p inhibition alleviates systemic sclerosis by targeting STAT3 signaling. *Journal of Translational Medicine* **22(1)**:323 DOI 10.1186/s12967-024-05056-3.

Patel A, Yang H, Douglas RS. 2019. A new era in the treatment of thyroid eye disease. *American Journal of Ophthalmology* **208(4)**:281–288 DOI 10.1016/j.ajo.2019.07.021.

Rajabi S, Saberi S, Najafipour H, Askaripour M, Rajizadeh MA, Shahraki S, Kazeminia S. 2024. Interaction of estradiol and renin-angiotensin system with microRNAs-21 and -29 in renal fibrosis: focus on TGF-β/smad signaling pathway. *Molecular Biology Reports* **51(1)**:137 DOI 10.1007/s11033-023-09127-4.

Seyhan AA. 2024. Trials and tribulations of microRNA therapeutics. *International Journal of Molecular Sciences* **25(3)**:1469 DOI 10.3390/ijms25031469.

Shahraki K, Pak VI, Najafi A, Shahraki K, Boroumand PG, Sheervalilou R. 2023. Non-coding RNA-mediated epigenetic alterations in Grave's ophthalmopathy: a scoping systematic review. *Non-coding RNA Research* **8(3)**:426–450 DOI 10.1016/j.ncrna.2023.04.001.

Shen L, Huang F, Ye L, Zhu W, Zhang X, Wang S, Wang W, Ning G. 2015. Circulating microRNA predicts insensitivity to glucocorticoid therapy in Graves' ophthalmopathy. *Endocrine* **49(2)**:445–456 DOI 10.1007/s12020-014-0487-4.

Song L, Feng S, Yu H, Shi S. 2022. Dexmedetomidine protects against kidney fibrosis in diabetic mice by targeting miR-101-3p-Mediated EndMT. *Dose Response: A Publication of International Hormesis Society* **20(1)**:15593258221083486 DOI 10.1177/15593258221083486..

Sorisky A, Pardasani D, Gagnon A, Smith TJ. 1996. Evidence of adipocyte differentiation in human orbital fibroblasts in primary culture. *The Journal of Clinical Endocrinology and Metabolism* **81(9)**:3428–3431 DOI 10.1210/jcem.81.9.8784110.

Sun H, Zhu R, Guo X, Zhao P, Zhang R, Zhao Z, Zhou H. 2024. Exosome miR-101-3p derived from bone marrow mesenchymal stem cells promotes radiotherapy sensitivity in non-small cell lung cancer by regulating DNA damage repair and autophagy levels through EZH2. *Pathology, Research and Practice* **256(5)**:155271 DOI 10.1016/j.prp.2024.155271.

Taylor PN, Zhang L, Lee RWJ, Muller I, Ezra DG, Dayan CM, Kahaly GJ, Ludgate M. 2020. New insights into the pathogenesis and nonsurgical management of Graves orbitopathy. *Nature Reviews Endocrinology* **16(2)**:104–116 DOI 10.1038/s41574-019-0305-4.

Wang H, Atkins SJ, Fernando R, Wei RL, Smith TJ. 2015. Pentraxin-3 is a TSH-inducible protein in human fibrocytes and orbital fibroblasts. *Endocrinology* **156(11)**:4336–4344 DOI 10.1210/en.2015-1399.

Wang N, Hou SY, Qi X, Deng M, Cao JM, Tong BD, Xiong W. 2021. LncRNA LPAL2/miR-1287-5p/EGFR axis modulates TED-derived orbital fibroblast activation through cell adhesion factors. *The Journal of Clinical Endocrinology and Metabolism* **106(8)**:e2866–e2886 DOI 10.1210/clinem/dgab256.

Wang S, Ren Y, Li J, Li H, Li J, Lan X, Wang Y. 2024. MicroRNA-671-5p regulates the inflammatory response of periodontal ligament stem cells via the DUSP8/p38 MAPK pathway. *Molecular Biology Reports* **51(1)**:644 DOI 10.1007/s11033-024-09510-9.

Wei H, Guan M, Qin Y, Xie C, Fu X, Gao F, Xue Y. 2014. Circulating levels of miR-146a and IL-17 are significantly correlated with the clinical activity of Graves' ophthalmopathy. *Endocrine Journal* **61(11)**:1087–1092 DOI 10.1507/endocrj.EJ14-0246.

Wiersinga WM, Bartalena L. 2002. Epidemiology and prevention of Graves' ophthalmopathy. *Thyroid: Official Journal of the American Thyroid Association* **12(10)**:855–860 DOI 10.1089/105072502761016476.

Woeller CF, Roztocil E, Hammond C, Feldon SE. 2019. TSHR signaling stimulates proliferation through PI3K/Akt and induction of miR-146a and miR-155 in thyroid eye disease orbital fibroblasts. *Investigative Ophthalmology & Visual Science* **60(13)**:4336–4345 DOI 10.1167/iovs.19-27865.

Xie B, Xiong W, Zhang F, Wang N, Luo Y, Chen Y, Cao J, Chen Z, Ma C, Chen H. 2023. The miR-103a-3p/TGFBR3 axis regulates TGF-β-induced orbital fibroblast activation and fibrosis in thyroid-eye disease. *Molecular and Cellular Endocrinology* **559**:111780 DOI 10.1016/j.mce.2022.111780.

Xu Y, Liu X, Cao J, Wu Y, Jiang Q, Luo B. 2024. Rho GTPase-activating protein 1 promotes hepatocellular carcinoma progression via modulation by CircPIP5K1A/MiR-101-3p. *Hepatology Research: The Official Journal of the Japan Society of Hepatology* **54(2)**:174–188 DOI 10.1111/hepr.13972.

Xue P, Huang S, Han X, Zhang C, Yang L, Xiao W, Fu J, Li H, Zhou Y. 2022. Exosomal miR-101-3p and miR-423-5p inhibit medulloblastoma tumorigenesis through targeting FOXP4 and EZH2. *Cell Death and Differentiation* **29(1)**:82–95 DOI 10.1038/s41418-021-00838-4.

Zhang H, Wang R, Wang Z, Wu W, Zhang N, Zhang L, Hu J, Luo P, Zhang J, Liu Z, Feng S, Peng Y, Liu Z, Cheng Q. 2022. Molecular insight into pentraxin-3: update advances in innate immunity, inflammation, tissue remodeling, diseases, and drug role. *Biomedicine & Pharmacotherapy* **156(1)**:113783 DOI 10.1016/j.biopha.2022.113783.

Zhao X, Li S, Wang Z, Bai N, Feng Y. 2021. miR-101-3p negatively regulates inflammation in systemic lupus erythematosus via MAPK1 targeting and inhibition of the NF-κB pathway. *Molecular Medicine Reports* **23(5)**:359 DOI 10.3892/mmr.2021.11998.

Zhao Q, Yang W, Li X, Yuan H, Guo J, Wang Y, Shan Z. 2023. MicroRNA-499-5p inhibits transforming growth factor-β1-induced Smad2 signaling pathway and suppresses fibroblast proliferation and collagen synthesis in rat by targeting TGFβ-R1. *Molecular Biology Reports* **50(12)**:9757–9767 DOI 10.1007/s11033-023-08755-0.